Available online at www.sciencedirect.com

ScienceDirect

Procedia Computer Science 95 (2016) 223 – 228

Procedia Computer Science

Complex Adaptive Systems, Publication 6
Cihan H. Dagli, Editor in Chief
Conference Organized by Missouri University of Science and Technology
2016 - Los Angeles, CA

Importance of Model Resolution on Discriminating Rapidly and Non-Rapidly Intensifying Atlantic Basin Tropical Cyclones

Andrew Mercer[a]*, Alexandria Grimes[a]

[a]*Northern Gulf Institute, 108 Hilbun Hall, Mississippi State University, Mississippi State, MS 39762*

Abstract

The ability to discriminate rapidly intensifying tropical cyclones (TCs) from their non-rapidly intensifying counterparts remains a major forecasting challenge in operational meteorology. Primarily, approaches to this forecast problem utilize dynamic model data as input into either numerical weather prediction models or statistical algorithms. Recent work suggested higher spatial resolution dynamic simulations will have greater success in distinguishing rapid intensification (RI) of TCs from those that do not, owing to the dynamic model's ability to depict smaller scale features explicitly within the simulation. Despite these preliminary findings, this approach has not been tested with a statistical modeling approach. As such, the scope of this work was to identify the importance of spatial resolution on the ability to forecast the onset of RI and non-RI TCs at 24 hour lead times. To accomplish this, 8 storms of each type were simulated using the Weather Research and Forecasting (WRF) model at varying spatial resolutions (54 km, 18 km, and 6 km). Meteorological fields from the WRF were used as input into a support vector machine classification algorithm trained to discriminate RI and non-RI TC environments.

Keywords: Tropical cyclones, principal component analysis, support vector machines

1. Introduction

The prediction of tropical cyclone rapid intensification remains a relevant forecast challenge in operational meteorology. Tropical cyclones (hereafter known as TCs) which undergo rapid intensification (RI) are consistently associated with the highest intensity storms, as all category 4 and 5 hurricanes and a vast majority of category 2-3 hurricanes undergo RI at least once in their evolution, and often multiple times [1]. As such, the threat to coastal locations from hurricanes which undergo RI is tremendous. Considerable work on forecasting RI [2-5] has suggested a series of predictors that are useful for distinguishing TCs that rapidly intensify from those that do not

doi:10.1016/j.procs.2016.09.318

(hereafter non-RI) with little forecast success (forecast skill scores less than 0.3). However, these approaches have been constrained to primarily linear regression techniques, despite the recent calls for artificial intelligence-based algorithms for distinguishing RI and non-RI storms. Preliminary studies into the application of AI techniques [1,5] have revealed some promise at reproducing model skill observed with the current operational implementation, but improvements using AI techniques above these current methods remain limited.

Recent work in numerical modeling of TCs has focused on the importance of higher resolution simulations when diagnosing RI. In particular, Chen and Gopalakrishnan [6] looked at the utility of the Hurricane Weather Research and Forecasting (HWRF) model to diagnose RI within Hurricane Earl (2010). They configured the HWRF with horizontal spatial resolutions of 27 km, 9 km, and 3 km, focusing specifically on the 3 km resolution results when diagnosing the onset of RI within the storm. Additional work utilizing the high-resolution HWRF model [7] has demonstrated potential value of the increases in resolution of the model, though HWRF coupling with an ocean model, and model parameterization configurations are likely affecting this improvement as well.

While the advantages of higher spatial resolution are clear when resolving smaller-scale processes within the TC, these simulations require considerable computing power and time for completion. Additionally, other research [2-4] has shown value in discriminating RI and non-RI TCs with lower spatial resolution prognostic fields. The current operational RI forecast model (the Statistical Hurricane Intensification Prediction Scheme Rapid Intensification Index – SHIPS-RII [2,3]) retains its peak forecast skill (Heidke Skill scores of roughly 0.2) with these lower resolution data. The SHIPS-RII is a multivariate linear regression scheme that has been blended into an ensemble approach, incorporating a Bayesian version of the model, a logistic regression, and a linear discriminant analysis. These techniques are limited by their inherent linearity, which could potentially be reducing forecast skill given the highly nonlinear meteorological relationships within a TC. The work of Grimes and Mercer [1,5] attempted to address this limitation through the introduction of a support vector machine (hereafter SVM) based classification scheme for RI/non-RI storms. Their work, while successful in achieving RI/non-RI discrimination skill on par with the current SHIPS-RII implementation (HSS of roughly 0.3, albeit in diagnostic mode), retains the spatial resolution limitations of the original SHIPS-RII studies [6,7].

To address this known deficiency, the goal of this project was to determine the ability of model forecasts to discriminate RI and non-RI storms relative to varied spatial resolutions of the input data. Discrimination was completed using a SVM (following [1,5]). The primary research hypothesis was that increases in spatial resolution in the model will yield improved classification ability by the SVM.

2. Data and Methods

2.1 Datasets

This project required a database of TCs with all associated intensification information. The National Hurricane Center (NHC) hurricane database (HURDAT) [8] contains 6 hourly TC position information, as well as peak wind gusts and central pressure. The current operationally implemented RI definition is an increase in peak wind speed of 30 kt in 24 hours, and this definition of RI is used in this study as well.

In addition to a database of TCs, meteorological fields were required for input in the Weather Research and Forecasting model (WRF model – [9]). While numerous global reanalysis databases exist, they are constrained with coarse spatial resolution (e.g. the NCEP/NCAR reanalysis [10] – 2.5° global resolution), meaning very few gridpoints would be available to resolve processes within TCs. To gain horizontal spatial resolution in the meteorological fields, a regional reanalysis was required. As such, the North American Regional Reanalysis (NARR – [11]) was selected as the input database for the model simulations. The NARR are provided from 1979-present every 3 hours on a Lambert-conformal grid centered on North America with 32 km grid spacing and 29 vertical levels. Unfortunately, the southeastern edge of the NARR domain (Fig. 1) extends very little into the southwestern Atlantic. This requires TC selection from the HURDAT to be constrained such that all storms maintained their entire track sufficiently within the NARR domain to capture relevant meteorological processes happing in the TC. This limited the study to a considerably smaller subset of candidate storms, resulting in 8 RI and 8 non-RI storms (Table 1) selected for the WRF simulations.

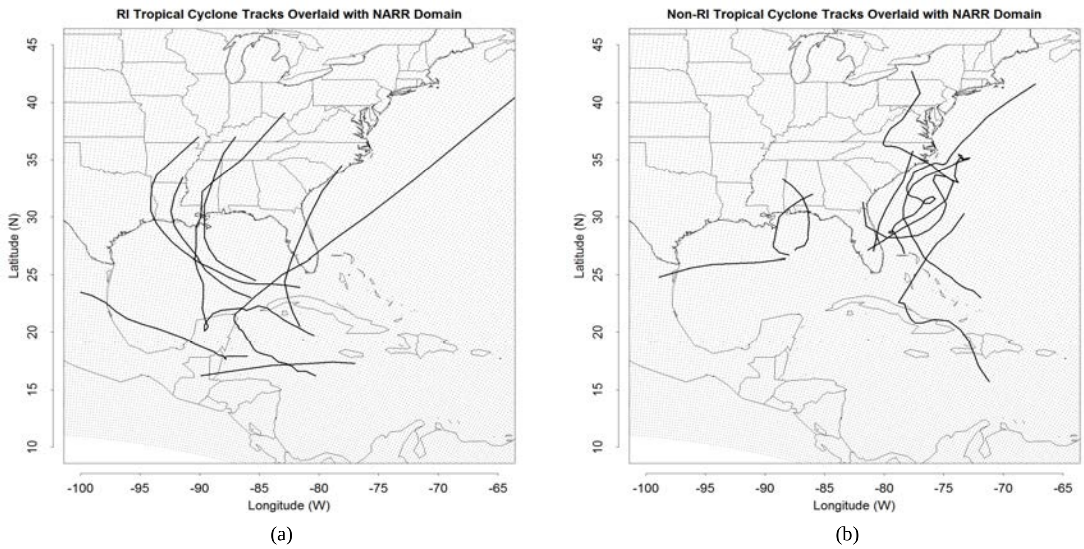

Fig. 1. Tracks for RI (panel a) and non-RI (panel b) storms included in the study. All tracks are fully encompassed within the NARR domain (given as a shaded region).

Table 1. List of the 16 tropical cyclones considered and their associated maximum intensification (in kt)

RI Storms		**Non-RI Storms**	
Storm Name/Year	Max Intensification	Storm Name/Year	Max Intensification
Keith 2000	65 kt	Godon 1994	20 kt
Iris 2001	45 kt	Dennis 1999	25 kt
Isidore 2002	40 kt	Barry 2001	25 kt
Lili 2002	35 kt	Hanna 2002	15 kt
Charley 2004	35 kt	Erika 2003	20 kt
Katrina 2005	60 kt	Ophelia 2005	20 kt
Rita 2005	50 kt	Ernesto 2006	25 kt
Wilma 2005	95 kt	Noel 2007	20 kt

2.2 WRF Model Setup

Once the 16 cases were selected, WRF model simulations at varied spatial resolutions were required. In this study, model parameterizations and vertical dimensions (45 vertical levels) were held constant for each horizontal resolution considered. The selected horizontal resolutions were scaled upward by a factor of 3 (54 km, 18 km, and 6 km) to ascertain the role of resolution on the simulations and subsequent classification ability over the same study domain (as seen in Fig. 1). All three simulations were completed for all 16 cases beginning at 36 hours prior to the time of most rapid deepening for each TC and continued for 12 hours after this peak intensification time (i.e., a 48 hour run time for each storm for each simulation). Integration timesteps were varied by resolution to reduce the likelihood of wave breaking (60 s at 54 km, 30 s at 18 km, and 15 s at 6 km). The selected study domain was uniform among all experiments (as seen in Fig. 1). The effects of the changes in resolution were clearly noted in the simulations, as considerable noise was introduced in the higher resolution simulations (e.g. Fig. 2 for mean sea level pressure from Hurricane Rita's simulation).

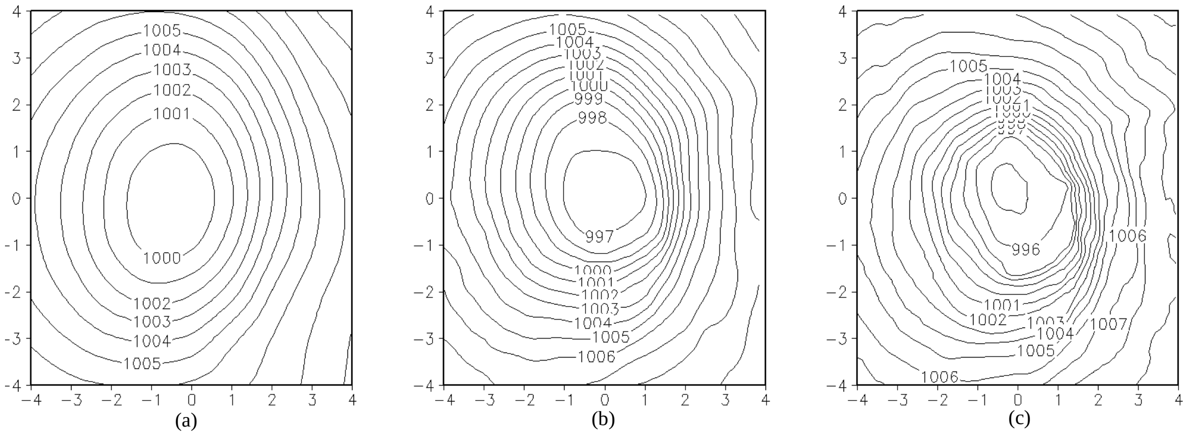

Fig. 2. Example of the influence of resolution on the WRF simulations. All three images are from Hurricane Rita at the time of peak intensification. Panel a shows the 54 km output, panel b the 18 km output, and panel c the 6 km output. All maps are positioned relative to the minimum sea level pressure of the hurricane (storm-centric).

The model configuration utilized, considered a common high-resolution HWRF configuration [6,7], included:

- WRF Single Moment 6-class (WSM6) microphysics scheme[12]
- Rapid Radiative Transfer Model for GCMs (RRTMG) shortwave and longwave radiation [13]
- Yonsei University Planetary Boundary Layer scheme [14]
- New Simplified Arakawa-Schubert cumulus scheme [15]
- Noah Land Surface model physics [16].

2.3 SVM Methodology

Building off of the work of [1] and [5], a SVM [17] was trained for distinguishing RI and non-RI TCs. As this is a forecasting study, the approach taken was in contrast with [1] and [5] in that each forecast time *prior to landfall* of its associated TC was classified as RI or non-RI by the SVM. This yielded 56 forecast times for the RI storms and 58 forecast times for the non-RI storms that were used as input into the SVM. Note that some simulations extended post-landfall; therefore, those timesteps were not included since RI is not forecasted once a storm makes landfall.

The WRF simulation fields used as input into the SVM included mean sea level pressure, sea surface (skin) temperature, 200 mb divergence, 500 mb vorticity, the magnitude of the 925 mb to 250 mb wind shear vector, and the equivalent potential temperature lapse rate at 700 mb. These fields encompass both kinematic characteristics within the TC (i.e. divergence, vorticity, and shear) and the thermodynamic properties of each storm (skin temperature, mean sea level pressure, and 700 mb equivalent potential temperature lapse rate). Grids of each field were retained for a roughly 500 km x 500 km grid centered on the TC at each resolution (9x9 grid at 54 km resolution, 23x23 grid at 18 km resolution, and 67x67 grid at 5 km resolution). Owing to the large number of spatial points for each simulation field and the large number of simulation fields utilized, a data reduction method was required prior to inputting the fields into the SVM as predictors. Data reduction was accomplished through an S-mode unrotated principal component analysis [1], where scree tests were used to determine the proper number of PCs to retain, with a minimum of 65% of variance explained kept by the retained PCs. This approach led to keeping 10 PCs for the 54 km data (total variance explained of 66.7%), 11 PCs for the 18 km data (total variance explained of 65.8%), and 13 PCs for the 6 km data (total variance explained of 65%). The PC scores were used as predictors in the SVM. Finally, to maintain consistency with the SHIPS-RII approach, the previous observation's (6 hours prior to the current observation) 24 hour wind speed change is used as a persistence predictor added to the PC scores from the meteorological fields.

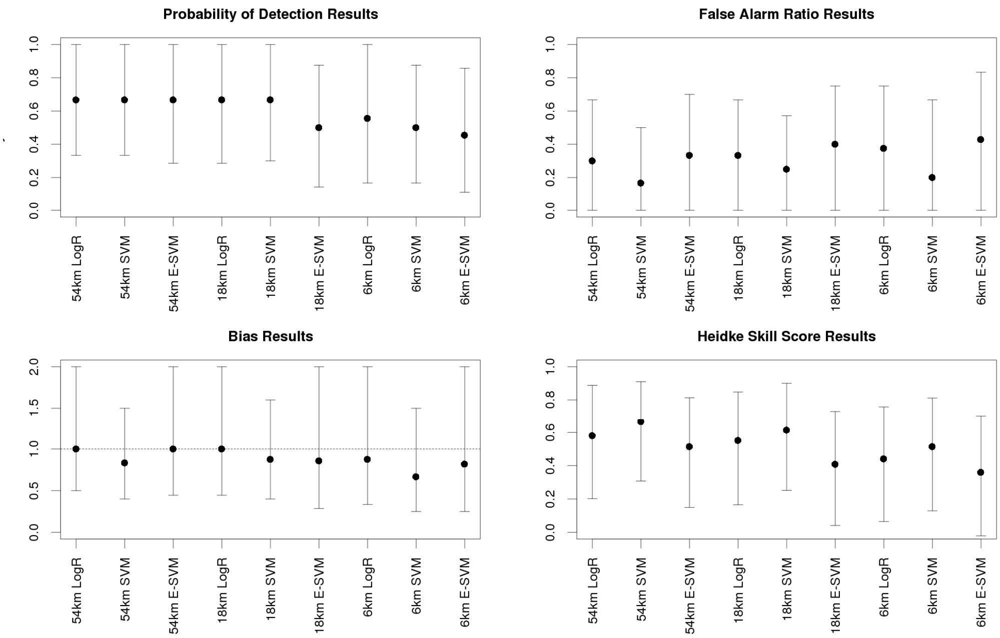

Fig. 3. Contingency statistics results for the baseline (logistic regression – LogR), the best performing SVM (labeled SVM), and the SVM ensemble (labeled E-SVM). The top left panel shows probability of detection (1 is perfect), the top right panel false alarm ratio (0 is perfect), the bottom left the bias (1 is unbiased as shown by the line), and the bottom right Heidke skill score (1 is perfect).

SVM cross-validation was completed uniformly among all 3 tested resolutions using a 5000-replicate bootstrap *k*-fold approach where 75% of the WRF simulated timesteps were withheld as training (randomly) and the remaining 25% of the timesteps were utilized as independent testing data. In this study, the measure of forecast performance was based on the probability of detection (hereafter POD) for an RI, the false alarm ratio (hereafter the FAR), and the Heidke skill score (hereafter the HSS) [5], which is a measure of forecast skill relative to a baseline climatology. Bias statistics are provided as well to assess over/under prediction of RIs. The bootstrap results were used to identify the SVM configuration with the best classification performance of those tested. The SVM configurations tested included radial basis function kernels (γ=0.1, 0.05, and 0.01) and polynomial kernels of degree 2, 3, 4, and 0.5. Cost functions were allowed to vary between 1 and 1000 by $\log_{10}$ units. All possible permutations (28 total SVM configurations) were tested at each resolution to identify optimal performance. Additionally, a second SVM utilizing the 28 SVM output results as input (an SVM-ensemble approach) was created using a SVM configuration identical to the best configuration of the 28 tested. Logistic regression was also tested as a baseline.

3. Results

The performance results (Fig. 3) revealed several interesting patterns in the classifications. Consistently, the best performing SVM (highest bootstrap median HSS) configuration was the radial basis function kernel with γ=0.01 and a cost of 10 (this configuration was used for the ensemble). There was a notable bump in HSS (though not statistically significantly better) associated with the optimal SVM configuration, with an HSS of 0.66 for SVM at 54 km versus 0.57 for logistic regression at the same resolution (results were similar for other resolutions). The ensemble SVM approach and the best performing SVM slightly underpredicted RIs (median bias statistics near 0.8 for 18 and 6 km simulations, unbiased at 54 km), while logistic regression maintained fairly unbiased predictions of RI. A result of particular note was the significant reduction in FAR associated with the SVM configuration of the model, all while retaining high POD and leading to a bump in HSS. This is an encouraging result, as FAR within forecasts is particularly problematic and reduction of FAR, while maintaining a high POD, is a relevant forecasting goal within RI prediction research. While the FAR reduction with the SVM was promising, the significant increase in FAR associated with the ensemble approach was discouraging. The ensemble approach yielded too many forecasted RIs when none occurred, despite being an underpredicting model for RIs, meaning many RI predictions were not correct. This also was seen in the relative decrease in POD for the ensemble approach, particularly at 18 and 6 km. It is important to note that the approach also yielded improvements of over 100% in HSS relative to the SHIPS-RII currently used operationally.

While the identification of the best technique for classification was important, the primary objective of this study was a diagnosis of the ability to classify RI and non-RI storms based on model resolution. The expectation based on previous research was that the highest resolution simulations would yield the greatest forecasts; however, the results of this study contrast those results directly, as the lowest resolution (54 km) simulations maintained the highest HSS values for all three modeling techniques portrayed in Fig. 3. Additionally, the 18 km and 6 km simulations maintained very similar HSS values despite the significant increase in spatial resolution (a slight drop in skill is observed in the 6 km results). Evidently, higher resolution simulations hinder classification skill for RI and non-RI TCs, possibly due to their inherent higher degree of noise (e.g. Fig. 2).

4. Conclusions

The objectives of this study were to identify the role of spatial resolution on classification ability between RI and non-RI TCs. The results were in contrast with expectation, as higher resolution simulations yielded lower forecast skill (though not statistically significantly so) versus lower resolutions, primarily owing to the lower probability of detection in the high resolution simulations. Many factors could have influenced these results, the most important of which are likely simulation quality and noisy fields. Future work will expand this database and consider differing lead times of the simulations, as well as considering convection-allowing high-resolution simulations (4 km or higher resolution). However, this first attempt reveals little benefit from high resolution simulations when predicting RI.

Acknowledgements: This work was funded by NOAA-OAR grant #NA11OAR4320199.

References

1. Mercer, A., Grimes, A. Diagnosing tropical cyclone rapid intensification using kernel methods and reanalysis datasets. *Prodcedia Comp. Sci.* 2015:**61**:422-7.
2. DeMaria, M., and Kaplan, J. A statistical hurricane intensity prediction scheme for the Atlantic basin. *Wea. Forecasting* 1993:**9**:209-20.
3. Kaplan, J., DeMaria, D. Large-scale characteristics of rapidly intensifying tropical cyclones in the North Atlantic basin. *Wea. Forecasting*, 2003:**18**:1093-108
4. Kaplan, J., Rozoff, C., DeMaria, D., Sampson, C., Kossin, J., Velden C., Cione J., Dunion, J., Knaff, J. Zhang, J., Dostalek J. Evaluating environmental impacts on tropical cyclone rapid intensification predictability utilizing statistical models. *Wea. Forecasting*, 2015:**30**:1374-96.
5. Grimes, A., Mercer, A. Synoptic-scale precursors to tropical cyclone rapid intensification in the Atlantic Basin. *Adv. Meteor.*, 2015:**1:**16pp.
6. Chen, H., and Golpalakrishnan, S. A study on the asymmetric rapid intensification of Hurricane Earl (2010) using the HWRF system. *J. Atmos. Sci.* 2015:**72**:531-550.
7. Tallapragada, V., Kieu, C., Kwon, Y., Trahan, S., Liu, Q., Zhang, Z., Kwon, I. Evaluation of storm structure from the operational HWRF during 2012 implementation. *Mon. Wea. Rev.* 2014:**142**:4308-4325.
8. Landsea, C., Franklin, J., Atlantic hurricane database uncertainty and presentation of a new database format. *Mon. Wea. Rev.*, 2013:**141**:3576-3592.
9. Skamarock, W., and coauthors. A description of the Advanced Research WRF Version 3. *NCAR Tech. Note* , Boulder, CO, 2008, 125pp.
10. Kalnay, E., and co-authors. The NCEP/NCAR 40-year reanalysis project. *Bull. Amer. Soc.* 1996:**77**:437-471.
11. Mesinger, F., and co-authors. North American Regional Reanalysis. *Bull. Amer. Soc.*, 2006:**87**:343-360.
12. Hong, S., J. Lim. The WRF single-moment 6-class microphysics scheme (WSM6). *J. Korean Meteor. Soc.*, 2006:**42**:129-151.
13. Iacono, M., Delamere, J., Mlawer, E., Shephard, M., Clough, S., Collins, W. Radiative forcing by long-lived greenhouse gases: Calculations with the AER radiative transfer models. *J. Geophysical Res.*, 2008:**113**:8 pp.
14. Hong, S., Noh, Y., Dudhia, J. A new vertical diffusion package with an explicit treatment of entrainment processes. *Mon. Wea. Rev*, 2006**:134**:2318-2341.
15. Han, J., H. Pan, R. Revision of convection and vertical diffusion schemes in the NCEP Global Forecast System. *Wea. Forecasting*, 2011:**26**:520-533.
16. Ek., M., and coauthors. Implementation of Noah land surface model advances in the National Center for Environmental Prediction operational mesoscale Eta model. *J. Geophys. Res.*, 2003:**108**:16pp.
17. Cristianini, N., and Shawe-Taylor, J. *An Introduction to Support Vector Machines and other Kernel-Based Learning Methods.* Cambridge University Press, Cambridge, England, 2000, 189 pp.